THE JOURNAL OF BIOLOGICAL CHEMISTRY
Vol. 275, No. 47, Issue of November 24, pp. 36974–36983, 2000
Printed in U.S.A.

Structure of C42D *Azotobacter vinelandii* FdI

A Cys-*X*-*X*-Asp-*X*-*X*-Cys MOTIF LIGATES AN AIR-STABLE [4Fe-4S]$^{2+/+}$ CLUSTER*

Received for publication, June 7, 2000, and in revised form, August 22, 2000
Published, JBC Papers in Press, August 28, 2000, DOI 10.1074/jbc.M004947200

Yean-Sung Jung‡, Christopher A. Bonagura‡, Gareth J. Tilley§, H. Samantha Gao-Sheridan‡¶, Fraser A. Armstrong§, C. David Stout‖, and Barbara K. Burgess‡**

From the ‡Department of Molecular Biology and Biochemistry, University of California, Irvine, California 92697, ‖Department of Molecular Biology, Scripps Research Institute, La Jolla, California 92037, and the §Department of Chemistry, Oxford University, Oxford OX1 3QR, United Kingdom

All naturally occurring ferredoxins that have Cys-*X*-*X*-Asp-*X*-*X*-Cys motifs contain [4Fe-4S]$^{2+/+}$ clusters that can be easily and reversibly converted to [3Fe-4S]$^{+/0}$ clusters. In contrast, ferredoxins with unmodified Cys-*X*-*X*-Cys-*X*-*X*-Cys motifs assemble [4Fe-4S]$^{2+/+}$ clusters that cannot be easily interconverted with [3Fe-4S]$^{+/0}$ clusters. In this study we changed the central cysteine of the Cys^{39}-*X*-*X*-Cys^{42}-*X*-*X*-Cys^{45} of *Azotobacter vinelandii* FdI, which coordinates its [4Fe-4S]$^{2+/+}$ cluster, into an aspartate. UV-visible, EPR, and CD spectroscopies, metal analysis, and x-ray crystallography show that, like native FdI, aerobically purified C42D FdI is a seven-iron protein retaining its [4Fe-4S]$^{2+/+}$ cluster with monodentate aspartate ligation to one iron. Unlike known clusters of this type the reduced [4Fe-4S]$^{+}$ cluster of C42D FdI exhibits only an S = 1/2 EPR with no higher spin signals detected. The cluster shows only a minor change in reduction potential relative to the native protein. All attempts to convert the cluster to a 3Fe cluster using conventional methods of oxygen or ferricyanide oxidation or thiol exchange were not successful. The cluster conversion was ultimately accomplished using a new electrochemical method. Hydrophobic and electrostatic interaction and the lack of Gly residues adjacent to the Asp ligand explain the remarkable stability of this cluster.

A fundamental question in [Fe-S] protein biochemistry concerns how cysteine ligand and neighboring residue organization determines [Fe-S] cluster type, and whether or not one type can be converted to another (for reviews, see Refs. 1–9). These issues are important, in part, because there are physiological situations where 3Fe to 4Fe or 4Fe to 2Fe cluster interconversion reactions modulate the activity of an enzyme or a regulatory protein (1, 8–13). In addition, understanding these reactions is of importance in attempts to create clusters with new reactivities (14), to the *de novo* design of [Fe-S]-containing proteins (14, 15), and to the study of [Fe-S] cluster assembly (16).

This study focuses on the simplest of these reactions, the interconversion of [3Fe-4S]$^{+/0}$ and [4Fe-4S]$^{2+/+}$ clusters. As shown in Fig. 1, these two cluster types differ only by the presence or absence of a single Fe atom at one corner of the cube. The well characterized seven-iron ferredoxin from *Azotobacter vinelandii*, which contains one [3Fe-4S]$^{+/0}$ and one [4Fe-4S]$^{2+/+}$ cluster, is proving to be an excellent model system for elucidating the properties of these redox centers. As shown in Fig. 2, the amino acid sequence Cys-*X*-*X*-Cys-*X*-*X*-Cys, which provides three of the four cysteine ligands to a [4Fe-4S]$^{2+/+}$ cluster, is a very common motif. Interestingly, with one exception, all naturally occurring ferredoxins or ferredoxin variants that contain 4Fe clusters, which can be easily interconverted with 3Fe clusters have instead a Cys-*X*-*X*-Asp-*X*-*X*-Cys motif. The Asp serves as the ligand that is lost during the cluster interconversion process (23, 25–29). The exception is *Dg*FdII where the central Cys is covalently modified in the [3Fe-4S] cluster-containing state and where the interconversion reaction is complicated by a change in subunit composition (10, 30). Aconitase, which also easily interconverts, also has a non-Cys (water or OH^-) ligand (31, 32). In contrast, for ferredoxins or variants that contain [4Fe-4S]$^{2+/+}$ clusters with four Cys ligands, attempts to convert the 4Fe center to a 3Fe center more often produce only poor yields or result in complete degradation accompanied by denaturation (33–38). This is certainly the case for the protein of interest in this study, *Av*FdI, where the oxidative destruction of its [4Fe-4S]$^{2+/+}$ cluster has been studied in some detail (38–40). In this study, we changed the central cysteine of the Cys^{39}-*X*-*X*-Cys^{42}-*X*-*X*-Cys^{45} motif, which coordinates the [4Fe-4S]$^{2+/+}$ cluster, into an aspartate. This paper describes the redox and spectroscopic properties of the new [4Fe-4S]$^{2+/+}$ cluster, and our various attempts to convert it into [3Fe-4S]$^{+/0}$. It also is the first report of the x-ray structure of an aspartate-liganded [4Fe-4S]$^{2+/+}$ cluster.

EXPERIMENTAL PROCEDURES

Mutagenesis and Expression of fdx—The oligonucleotide used for the mutagenesis has the sequence 5′-TGCATCGACGACGCGCTCTG-3′, which differs from the wild-type sequence by the substitution of TGC (encoding Cys) for GAC (encoding Asp). The oligonucleotide-directed mutagenesis procedure was similar to that previously described (41, 42) except that a pBluescript SK$^-$ phagemid was used as the mutagenesis vector instead of M13mp18. The mutation was confirmed at the DNA level by DNA sequencing. A 1.9-kilobase pair *Cla*I-*Xho*I fragment of *A. vinelandii* carrying wild-type *fdxA* gene was inserted into pBluescript SK$^-$. The fragment containing the mutation was subcloned into pKT230 as described elsewhere (43), and electroporation was used to

* This work was supported by National Institute of Health Grants GM-45209 (to B. K. B.) and GM-36325 (to C. D. S.) and by United Kingdom Engineering and Physical Sciences Research Council (EPSRC) and Biotechnology and Biological Sciences Research Council (BBSRC) Grant B11675 (to F. A. A.). The costs of publication of this article were defrayed in part by the payment of page charges. This article must therefore be hereby marked "*advertisement*" in accordance with 18 U.S.C. Section 1734 solely to indicate this fact.

The atomic coordinates and structure factors (code 1FF2) have been deposited in the Protein Data Bank, Research Collaboratory for Structural Bioinformatics, Rutgers University, New Brunswick, NJ (http://www.rcsb.org/).

¶ Current address: Dept. of Microbiology and Molecular Genetics, Harvard Medical School, Boston, MA 02115

** To whom correspondence should be addressed. Tel.: 949-824-4297; Fax: 949-824-8551; E-mail: bburgess@uci.edu.

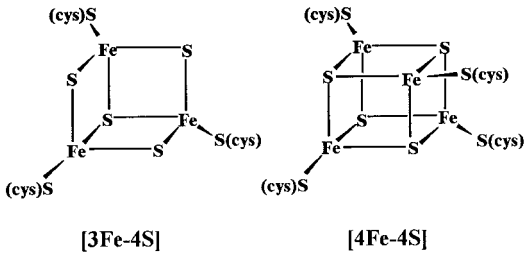

FIG. 1. **Structures of [3Fe-4S] and [4Fe-4S] clusters.** *S*, inorganic sulfide; *S (cys)*, cysteine.

$[4Fe\text{-}4S]^{2+/+}$ ligands	* * * #
*Cp*Fd	IADSCVSCGACASECPVNAIS
*Cp*Fd[1]	DADTCIDCGNCANVCPVGNPV
*Av*Fd	HPDECIDCALCEPECPAQAIF
Dv (Miyazaki)	DEEECLGCESCVEVCEAGAIT
*Da*FdIII	NEDECLGCESEVEVCEQDALT
*Sa*Fd	NEQACIFCMACVNVCPVAAID
*Ta*Fd	RESDCIFCMACESVCPVRAIK
3Fe/4Fe ligands	**# # # ***
Dv (Miyazaki)	DTDKCTGDGECVDVCPVEVYE
*Da*FdIII	DTDKCTGDGECVDVCPVEVYE
*Pf*Fd	DQDTCIGDAICASLCPDVFEM
*Sa*Fd	DFDLCIADGSCITACPVNVFQ
*Ta*Fd	DWDCCIADGACMDVCPVNLYE
*S7*Fd	DFDLCIADGSCINACPVNVFQ
*Dg*FdII	VNDDCMACEACVEICPDVFEM

FIG. 2. **Sequence comparison of examples of Cys motifs for the 4Fe clusters that do not interconvert (*top*) and 3Fe/4Fe interconversion motifs (*bottom*).** *Cp*Fd (*C. pasteurianum*, Ref. 17), *Av*Fd (*A. vinelandii,* Ref. 18), *Dv*Fd, Miyazaki (*Desulfovibrio vulgaris Miyazaki*, Ref. 19), *Da*FdIII (*Desulfovibrio africanus*, Ref. 20), *Sa*Fd (*Sulfolobus acidocaldarius*, Ref. 21), *Pf*Fd (*Pyrococcus furiosus*, Ref. 22), *Ta*Fd (*Thermoplasma acidophilum*, Ref. 23), *S7*Fd (*Sulfolobus sp.* strain 7, Ref. 24), and *Dg*FdII (*Desulfovibrio gigas* FdII, Ref. 10). The *superscript 1* indicates the second motif in the same protein.

introduce the plasmid into the *A. vinelandii* strain LM100, which contains a disruption of the *fdxA* gene by a kanamycin resistance cartridge.

Protein Purification—All *A. vinelandii* cells were grown under N_2-fixing conditions in a 200-liter New Brunswick fermentor (42). The protein purification was carried out at room temperature, and fractions were monitored by their absorbance at 405 nm and by cross-reactivity with antibodies raised against purified FdI, FdIII, or FdIV. The purification was carried out aerobically. Cell-free extracts were prepared from 1 kg of cells, and the first DEAE-cellulose column was run as described previously for the purification of other FdI variants (43). From the first DEAE-cellulose column, the FdI fraction eluted at 70–80% of the linear 0.1–0.5 M NaCl gradient (total volume = 3 liters) as a very shallow, yet well resolved brown peak. The protein fraction was immediately diluted with three volumes of 0.1 M potassium phosphate buffer, pH 7.4, and loaded onto a 2.5 × 20-cm DEAE-cellulose column that was preequilibrated with the same buffer. Following loading, the column was washed at the elution rate of 3.0 ml/min for 24 h with 0.12 M KCl in the same buffer until the greenish-brown FdIII (34) eluted. The brownish FdI with the red-colored FdIV (44), which was visible on the column immediately following FdIII, was then eluted with 0.3 M KCl. Ammonium sulfate was added slowly to 75% saturation with stirring. After a 30-min incubation, the sample was centrifuged at 20,000 × *g* for 20 min. The pellet was then collected and resuspended in 0.025 M Tris-HCl, pH 7.4, before loading onto a 1.5 × 110-cm Superdex G-75 (Amersham Pharmacia Biotech) column preequilibrated with 0.025 M Tris-HCl, pH 7.4, 0.1 M NaCl. The brown-colored C42D FdI protein and red-colored FdIV eluted as a single broad peak as observed by monitoring at 405 nm; however, the FdIV actually moved slightly faster than C42D FdI. For that reason, the last third of the peak was collected and concentrated using a Centriplus-10 concentrator (Amicon) prior to further purification on a 1-ml Mono-Q FPLC system (Amersham Pharmacia Biotech) with a flow rate of 1 ml/min and a linear gradient of 0.3–0.8 M NaCl in 0.05 M Tris-HCl, pH 8.0, over 20 ml. Two fractions were well resolved: the red-colored fraction (FdIV), which eluted between 0.46 and 0.48 M NaCl, and a brown-colored fraction (FdI), which eluted between 0.54 and 0.58 M NaCl. Each fraction was collected, buffer-exchanged with 0.025 M Tris-HCl, pH 7.4, and concentrated to 0.5 ml. The C42D protein fraction was further purified with triclinic crystallization. The yield for C42D FdI protein is ~ 0.5–1 mg/kg of cell paste.

Protein Characterization—To determine iron content, samples were digested, and the analysis was carried out as described previously (45) using $FeCl_3 \cdot 6H_2O$ to generate a standard curve with FdI and FdIII (34) as controls. EPR[1] spectra were obtained using a Bruker ESP300E spectrometer, interfaced with an Oxford liquid helium cryostat. For spin quantitation of $[3Fe\text{-}4S]^+$, the spectrum was recorded at 10 K using 100 μM purified C42D FdI at microwave power of 1 mW. Under those conditions, the EPR signal of FdI is linearly proportional to (microwave power)$^{1/2}$. 100 μM Cu^{2+}-EDTA, which was used as a standard, was recorded at the same EPR setting and temperature, where the signal is also linear with respect to (power)$^{1/2}$. The spin concentration was determined by double integration of the signal over the entire field sweep (46). For anaerobic EPR measurement, the samples were loaded into the EPR tubes in an O_2-free (O_2 < 1 ppm) glove box (Vacuum Atmosphere, Hawthorne, CA). The tubes were sealed with a cap, wrapped with parafilm, and then transferred to the liquid nitrogen Dewar flask. Reduction of FdI was carried out by mixing degassed FdI, 5-deazariboflavin and EDTA (final concentration, 0.2, 0.15, and 10 mM, respectively) in 0.05 M Tris-HCl, pH 8.0, and then illuminating the mixture for 1 min using white light from a fiber optics illuminator, model 20 (150 W, Edmond Scientific Co., Barringston, NJ) (34). Using this system, the extent of reduction of the $[4Fe\text{-}4S]^{2+}$ cluster of FdI depends upon the light intensity, light illumination time, media anaerobicity, and absence of other electron acceptors. Oxidation with $K_3Fe(CN)_6$ was carried out anaerobically in 0.05 M potassium phosphate buffer, pH 7.5; FdI was incubated at room temperature with $K_3Fe(CN)_6$ at a molar ratio of 1:3 for 2 h prior to freezing (39, 40). For NMR, samples were exchanged into a 0.05 M Tris-buffered D_2O solution, pH 7.8, by passage through a Sephadex G-25 column (1.5 × 15 cm). The FdI fraction was then concentrated to ~0.6–1.0 mM by microfiltration with a Centriprep-10 (Amicon, Beverly, MA). ^1H 500-MHz NMR spectra were recorded at room temperature using 90° pulses of 8 μs with 0.5-s delay times, using a Bruker GN-500 Fourier transform NMR spectrometer at the NMR facility, University of California, Irvine, CA. About 6000 scans were accumulated for each spectrum over a 2.5-h period. UV-visible absorption spectra were each recorded in a 0.5-ml quartz cuvette on a Hewlett Packard 8452A diode array spectrophotometer. CD spectra were obtained using a Jasco J-500C spectropolarimeter, with the sample contained in a small volume cylindrical cell with fused quartz window.

Electrochemistry—Purified water of resistivity ~ 18 megohm·cm^{-1} (Millipore, Bedford, MA) was used in all experiments. The buffers MES, HEPES, and TAPS and the co-adsorbates neomycin or polymyxin (sulfate salts) were purchased from Sigma. An AutoLab electrochemical analyzer (Eco Chemie, Utrecht, The Netherlands) was used to record DC cyclic voltammograms. All experiments were carried out under anaerobic conditions in a Vacuum Atmospheres glove box with an inert atmosphere of N_2 (<1 ppm). The three-electrode configuration featuring all-glass cells has been described previously (47); this featured a jacketed main cell compartment (typically holding 500 μl), which could be maintained at 0 °C to optimize protein film stability. The saturated calomel reference electrode was held in a Luggin side arm. Prior to each experiment, the pyrolytic graphite "edge" electrode (surface area typically 0.18 cm^2) was polished with an aqueous alumina slurry (Buehler Micropolish; 1.0 μm) and sonicated extensively to remove traces of Al_2O_3. Reduction potentials ($E^{0'}$) from cyclic voltammetry were determined from the average of the anodic and the cathodic peak potentials, $E^{0'} = \frac{1}{2}(E_{pa} + E_{pc})$ and adjusted to the standard hydrogen electrode scale using $E_{SCE} - E_{SHE} + 243$ mV at 22 °C (where SCE is saturated calomel reference electrode and SHE is standard hydrogen electrode).

Bulk electrochemistry solutions contained between 0.05 and 0.1 mM protein in 60 mM mixed buffer (15 mM HEPES, 15 mM MES, 15 mM TAPS, and 15 mM acetate), with 0.1 M NaCl as supporting electrolyte and 4 mM neomycin. Neomycin stabilizes the protein-electrode interactions. For film solution experiments, solution used to coat the electrode contained approximately 0.1 mM protein in 60 mM mixed buffer, 0.1 mM NaCl, and 200 μg/ml polymyxin at pH 7.0. The cell solution in each case was of similar composition but contained no protein and was adjusted to the required pH with either HCl or NaOH. The pH of the cell solution was measured before and immediately after the experiment. For detailed analysis, voltammograms were corrected for non-faradaic back-

[1] The abbreviations used are: EPR, electron paramagnetic resonance; Fd, ferredoxin; FPLC, fast protein liquid chromatography; MES, 2-(*N*-morpholino)ethanesulfonic acid; TAPS, *N*-tris(hydroxymethyl)methyl-3-aminopropanesulfonic acid; W, watt(s); T, tesla.

TABLE I
Crystallographic data for C42D FdI

Space group	$P4_12_12$
Unit cell (Å)	$a = 55.30$; $c = 90.59$
Data collection	All data (last shell)
Resolution (Å)	40.0–2.30 (2.34–2.30)
Total observations	48,416
Unique reflections	6,640
Completeness (%)	98.8 (99.7)
Rsymm (%)	0.171 (0.78)
$I/\sigma(I)$	11.8 (3.1)
Refinement	
Resolution (Å)	23.8–2.30
Reflections	6,320
R-factor	0.217
Rfree (5% of reflections)	0.269
Geometry	Root-mean-square deviations
Bonds (Å)	0.017
Angles (degrees)	2.64
Average *B*-factors (Å^2)	
Protein (atoms)	24.7 (843)
[Fe-S] clusters (atoms)	23.9 (15)
Solvent (H_2O molecules)	29.1 (48)

ground current by subtracting a polynomial base line (48). Pulsing experiments were carried out as follows. Films were prepared and then scanned over the normal potential range until the film had stabilized (usually three scans). This voltammogram was then recorded. The protein film was then subjected to an oxidative potential pulse of 0.643 V for 1–4 s. A scan was then taken immediately afterward in the normal potential region, in order to observe the changes that had occurred.

Crystallization—Crystals of C42DFdI were grown by the standard methods as described previously (49, 50). However, the protein appeared to denature quickly in drops that contained higher concentrations of ammonium sulfate. Touchseeding and attempts to macroseed did not work. Macroseeds quickly denatured when placed in preequilibrated drops. A few crystals grew spontaneously after several months' incubation at 4 °C and appeared to be small but regular. These crystals grew in only two of all the drops seeded.

Attempts to cryoprotect these crystals did not work. The crystals quickly melted when placed in ammonium sulfate saturated drop buffer supplemented with 20% or 25% glycerol. As a result, after several failed attempts to mount a crystal, the crystal used for data collection was scooped directly out of the drop conditions and frozen in the N_2 cryostream without cryoprotectant.

Structure Determination—The structure of native FdI was modeled with a glycine at position 42, and refined by rigid body and positional refinement against all of the data to 2.3-Å resolution (Table I) using Xplor version 3.8 (51). The unbiased $2|F_o| - |F_c|$ and $|F_o| - |F_c|$ electron density maps clearly revealed the position of the Asp^{42} side chain with very little other perturbation in the structure. The Asp^{42} side chain was modeled into the density with Xfit/Xtalview (52), and the structure was refined with isotropic *B*-factors and a bulk solvent correction using Xplor version 3.8. The Asp^{42} side chain was restrained to form a 2.1-Å bond to Fe of the [4Fe-4S] cluster, as indicated by the density. The refined model was checked and adjusted against a 2.3-Å resolution $2|F_o| - |F_c|$ map. A $|F_o| - |F_c|$ map was used to locate well ordered H_2O molecules, which were included in the model and refined. Statistics for the final model are summarized in Table I. Coordinates have been deposited with the Protein Data Bank with accession number 1FF2.

RESULTS AND DISCUSSION

Cell Growth and Protein Purification—A. vinelandii is a nitrogen-fixing soil bacterium that appears to synthesize at least 12 different ferredoxins (44). FdI is the only seven-iron ferredoxin that has been identified in that organism. Previous studies have established that FdI has a regulatory function as part of an oxidative stress response system in *A. vinelandii* (53–58) and a metabolic function unrelated to nitrogen fixation that is important for cell growth (59). Mutagenesis experiments have shown that even subtle alterations in the environment of the $[3Fe\text{-}4S]^{+/0}$ cluster have profound negative effects on the growth rate of the organism (42). In contrast, much more drastic alterations in the environment of the $[4Fe\text{-}4S]^{2+/+}$ cluster have no effect on cell growth (60). In keeping with these observations, the *A. vinelandii* strain expressing C42D FdI and the strain expressing native FdI exhibit identical lag phases and growth rates.

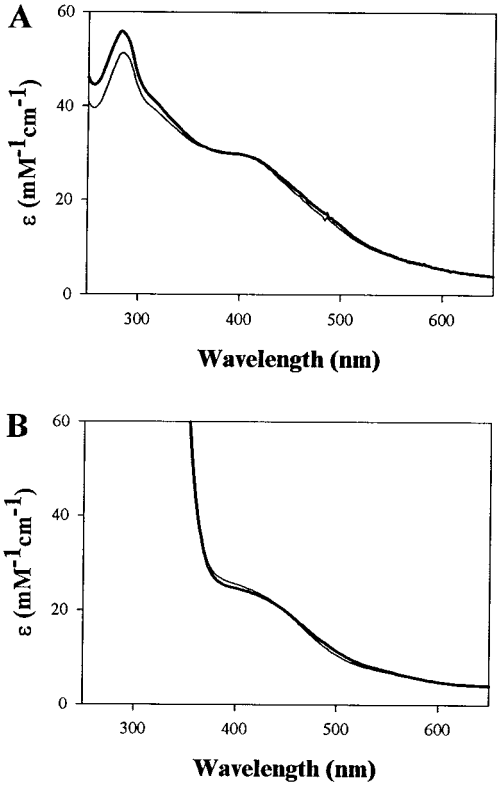

FIG. 3. **UV-visible absorption spectra of air-oxidized (*A*) and reduced (*B*) C42D and native FdI.** *Thin line*, native FdI; *thick line*, C42D FdI. The samples were reduced with 2 mM sodium dithionite for 1 h in 0.050 M Tris-HCl, pH 8.0, and 0.1 M NaCl.

Previous studies have also shown that mutations involving FdI [Fe-S] cluster ligands always lead to proteins that accumulate to much lower levels *in vivo* than does the native protein (41, 61). This is also true for C42D FdI. Despite the low levels of accumulation of the C42D FdI *in vivo*, however, once the protein is purified it appears to be as stable as native FdI. What is particularly important for this study is the fact that the protein is completely stable toward oxygen.

Like Native FdI, C42D FdI Is a Seven-iron Protein—Native *Av*FdI contains one $[4Fe\text{-}4S]^{2+/+}$ cluster and one $[3Fe\text{-}4S]^{+/0}$ cluster (49, 62, 63). The C42D mutation in *Av*FdI converted the central cysteine of the $[4Fe\text{-}4S]^{2+/+}$ binding motif, Cys^{39}-*X*-*X*-Cys^{42}-*X*-*X*-Cys^{45}, to an aspartate. Naturally occurring ferredoxins that contain Cys-*X*-*X*-Asp-*X*-*X*-Cys motifs assemble $[4Fe\text{-}4S]^{2+/+}$ clusters that are easily converted by air oxidation to $[3Fe\text{-}4S]^{+/0}$ clusters (10, 19–24); this was the expected outcome in this case. We were therefore surprised to observe that the UV-visible absorption spectrum of the air-oxidized C42D FdI was nearly identical to that of the native FdI (Fig. 3), suggesting that the protein retained its original cluster composition. Oxidized $[3Fe\text{-}4S]^{+}$ clusters exhibit characteristic $g = 2.01$ EPR signals that integrate to one spin per molecule. If air-oxidized C42D FdI contained two $[3Fe\text{-}4S]^{+}$ clusters, then we would expect the size of its EPR signal to double, integrating to two spins per molecule. In contrast, as shown in Fig. 4, the EPR spectrum of air oxidized C42D FdI exhibits a $g = 2.01$ signal, similar in shape and size to that of native FdI, which is again consistent with its retaining the original cluster composition. Iron analysis was used to confirm that C42D FdI had not lost an iron to become a 6Fe-containing protein, and a value of

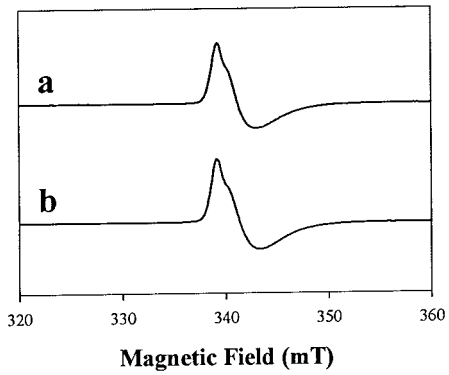

FIG. 4. **X-band EPR spectra of air-oxidized native (*a*) and C42D (*b*) FdI.** Both samples were 40 μM in 0.050 M Tris-HCl, pH 8.0, 0.1 M NaCl. Conditions of measurements: microwave frequency, 9.59 GHz; modulation amplitude, 0.64 mT; microwave power, 1 mW; temperature, 10 K; receiver gain, 5×10^3.

7.5 ± 0.4 iron atoms/molecule for C42D FdI was obtained. That the cluster composition of air oxidized C42D FdI is identical to that of native FdI was subsequently confirmed by x-ray crystallography.

The [4Fe-4S]$^{2+/+}$ Cluster of C42D FdI Has Only Three Cysteine Ligands—For reference, Fig. 5 shows the [4Fe-4S]$^{2+/+}$ region of native FdI. In general, [4Fe-4S]$^{2+/+}$ clusters like the one in native FdI obtain three of their four cysteine ligands from a Cys-*X*-*X*-Cys-*X*-*X*-Cys sequence, whereas the fourth cysteine ligand comes from a remote part of the protein, in this case Cys^{20}. As shown in Fig. 5 there is also a fifth free cysteine (Cys^{24}) in van der Waals contact with the [4Fe-4S]$^{2+/+}$ cluster of native FdI. Previous studies have shown that both C20A (64) and C20S (50) variants of FdI assemble [4Fe-4S] clusters with four cysteine ligands by recruiting Cys^{24}. In order to use that cysteine as a new ligand, polypeptide rearrangements were necessary in both cases (50, 64). For the C42D mutant, we wanted to address the possibility that the [4Fe-4S]$^{2+/+}$ cluster might ignore the introduced aspartate and assemble instead using the four cysteine residues Cys^{20}, Cys^{24}, Cys^{39}, and Cys^{45}.

In general, visible region CD spectroscopy is very sensitive to the type of [Fe-S] cluster a protein contains. As shown in Fig. 6, oxidized native FdI exhibits a distinctive CD spectrum with contributions from both clusters. Previous studies have shown that both the wavelength dependence and form of this spectrum is dramatically changed for both the C20A and C20S variants, each of which undergo ligand exchange and structural rearrangement (50, 64). In contrast, as shown in Fig. 6, the CD spectrum of oxidized C42D FdI is similar in wavelength dependence and form to that of native FdI. These data argue against a ligand exchange with an accompanied structural rearrangement.

Further support for the conclusion that [4Fe-4S]$^{2+/+}$ cluster of C42D FdI does not recruit the free cysteine at position 24 (Fig. 5) as a new ligand comes from studies of the oxidation of the protein by ferricyanide. Previous studies have established that native FdI reacts with $Fe(CN)_6^{3-}$ in a three-step degradative process in which the first step is a three-electron oxidation, involving the [4Fe-4S]$^{2+/+}$ cluster and giving rise to a paramagnetic species (39, 40). As shown in Fig. 7, this exhibits EPR up to quite high temperature and is most easily monitored in the range 40–60 K (*c* and *d*), where the [3Fe-4S]$^{+}$ cluster EPR is not detectable (*a* and *b*) (39, 40). It has been established that this reaction absolutely requires a free cysteine at position 24 and the paramagnetic species is not observed for a C24A variant or for the C20A variant that has rearranged to utilize C24 as a new ligand (61). Fig. 7 shows that the behavior of C42D FdI is indistinguishable from that of native FdI in this reaction,

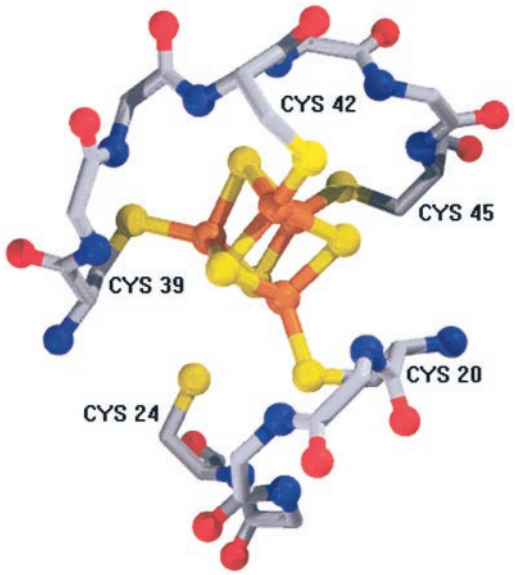

FIG. 5. **The structure of native FdI in the vicinity of the [4Fe-4S]$^{2+}$ cluster showing the main chain atoms of residues 20–24 and 39–45, and the side chains of all four Cys ligands as well as that of the non-ligand residue Cys^{24}.**

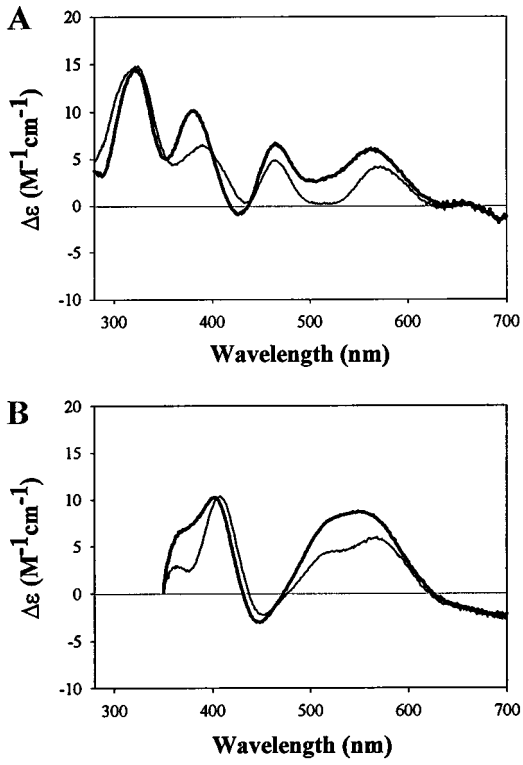

FIG. 6. **Visible region CD spectra of air-oxidized (*A*) and reduced (*B*) state of C42D and native FdI.** *Thin line*, native FdI; *thick line*, C42D FdI. The FdI in the reduced state was made by addition of 2 mM sodium dithionite for 2 h into FdI sample. The samples were suspended in 0.050 M Tris-HCl, pH 8.0, 0.1 M NaCl.

confirming that C24 remains free in this variant. Taken together, the CD and the ferricyanide oxidation experiments lead to the conclusion that in solution the [4Fe-4S]$^{2+/+}$ cluster of C42D FdI is ligated by only three cysteine residues.

Aspartate Ligation Is Confirmed by X-ray Crystallography—Prior to this report, there were no x-ray structures available for any [4Fe-4S] clusters with aspartate ligation. After 2 years of trying, and only after the original version of this paper had been submitted, we were finally successful in obtaining diffrac-

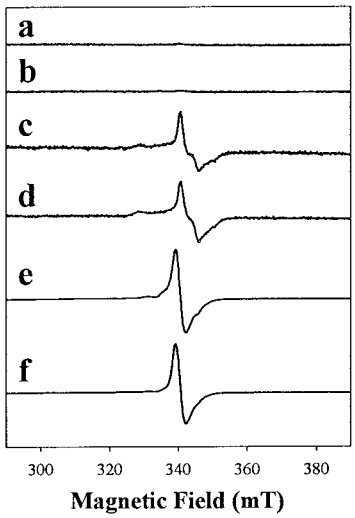

FIG. 7. **X-band EPR spectra of native (*a*, *c*, and *e*) and C42D (*b*, *d*, and *f*) FdI either not treated (*a* and *b*) or treated (*c–f*) with 3 equivalents of $K_3Fe(CN)_6$.** The samples were 40 μM in 0.050 M Tris-HCl, pH 8.0, 0.1 M NaCl. The EPR measurements were made in either 30 K (*a–d*) or 10 K (*e* and *f*). The rest condition of measurements: microwave frequency, 9.59 GHz; modulation amplitude, 0.64 mT; microwave power, 1 mW; receiver gain, 2×10^4 for *a–d*, 5×10^3 for *e* and *f*.

tion quality crystals of C42D FdI. As expected from the spectroscopy, the structure of C42D FdI is very similar to native FdI with Asp^{42} superposing closely on Cys^{42}. The root-mean-square deviation of all main chain atoms in the two structures is 0.27 Å following least squares superposition. The main chain is displaced outward by 0.27 Å at the Cα of residue 42 due to the mutation. There is a similar small displacement of the Pro^{21} and Leu^{44} side chains, and at Cys^{45} as well. Overall the electron density for residues 39–45 is well defined in C42D FdI, and these residues have comparable *B*-factors to the native protein, except for Leu^{44}, which has significantly weaker density for its side chain.

In C42D FdI the Oδ2 atom of Asp^{42} is located within ~0.2 Å of the position of Sγ in the native protein, and so it is able to form a covalent bond, 2.11 Å in length, with Fe of the [4Fe-4S] cluster (Fig. 8*A*). In this orientation of the side chain, the Oδ1 atom is farther from Fe, at 3.14 Å; therefore, Asp^{42} acts as a monodentate ligand. It is important to note that the orientation of Asp^{42} in Fig. 8*A*, with Oδ1, Oδ2 to Fe distances of 3.14 and 2.11 Å, respectively, is not the same orientation as the bidentate orientation proposed for the [4Fe-4S](Cys_3Asp) cluster of *P. furiosus* Fd based on an nuclear magnetic resonance (NMR) structure (28) or for a [4Fe-4S] model complex with three thiolate ligands and one carboxylate ligand (65). Insertion of the aspartate side chain into the cluster-binding loop results in three short contacts to adjacent hydrophobic residues (Fig. 8*A*). These involve the Oδ1 atom with Cγ1 of Ile^{40} and Cγ of Pro^{21}, and the Oδ2 atom with Cβ of Leu^{44}. The tight packing of these three hydrophobic residues around the Asp^{42} side chain is illustrated in Fig. 8*B* and will be discussed below.

Direct Comparison of the Properties of the Oxidized [4Fe-4S]$^{2+}$ Clusters of C42D and Native FdI—Fig. 3 compares the UV-visible absorption spectra of air oxidized (*A*) and dithionite-reduced (*B*) C42D and native FdI. Because of its very low reduction potential, the [4Fe-4S]$^{2+/+}$ cluster in FdI remains oxidized in the presence of dithionite, while the [3Fe-4S]$^{+/0}$ cluster is reduced. The similarity of spectra between native and C42D in both the oxidized and reduced states confirms that there is no major structural rearrangement due to the C42D mutation.

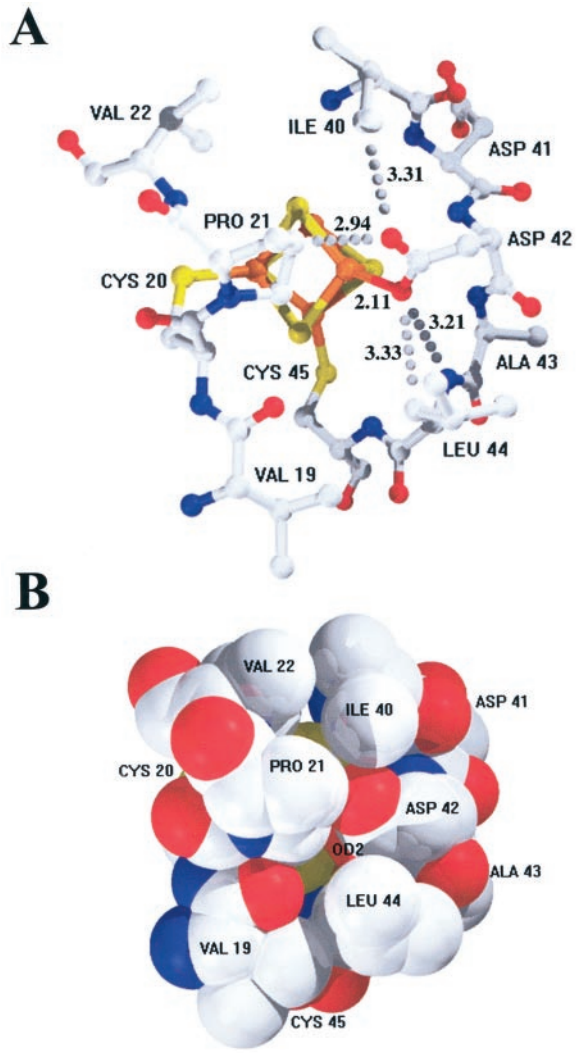

FIG. 8. **X-ray crystal structure of [4Fe-4S] cluster regions in C42D FdI.** The view is similar to that in Fig. 5. Atoms are colored as follows: Fe, *orange*; S, *yellow*; O, *red*; N, *blue*; C, *gray*. *A*, all atoms of residues 19–22 and 40–45, and the [4Fe-4S] cluster, are shown. *Dotted lines* indicate short hydrophobic contacts of Asp^{42} with amino acid residues Pro^{21}, Ile^{40}, and Leu^{44}, and hydrogen bonds between Oδ1 of Asp^{42} and Pro^{21} and between Oδ2 of Asp^{42} and the amide of Leu^{44}. *B*, same view as in *A* with all atoms of residues 19–22 and 40–45, and the cluster, rendered as spheres with radii corresponding to van der Waals radii. Short contacts between oxygen atoms of the Asp^{42} side chain include 3.31 Å to Cγ1 of Ile^{40} and 3.33 Å to Cβ of Leu^{44}.

The wavelength dependence and form of the visible region CD spectra exhibited by different [Fe-S] proteins is not only sensitive to cluster type and protein environment but also changes substantially upon oxidation and reduction. Fig. 6*B* compares the CD spectra exhibited by dithionite-reduced C42D and native FdI. Again, the [4Fe-4S]$^{2+/+}$ cluster remains oxidized under these conditions. The similarity of the wavelength dependence and overall shape of the spectrum confirm that there is no major structural change occurring upon reduction of the [3Fe-4S]$^{+}$ cluster. The small changes in form of the reduced spectrum likely arise from the Cys to Asp change in ligation for the [4Fe-4S]$^{2+}$ cluster.

The ^{1}H NMR spectrum of oxidized native *Av*FdI shows several well resolved, paramagnetically shifted resonances (66). The five most downfield resonances are shown in Fig. 9. Three of these, designated A–C, have previously been assigned to the methylene protons of cysteine ligands to the [3Fe-4S]$^{+}$ cluster, while the other two are believed to arise from methylene pro-

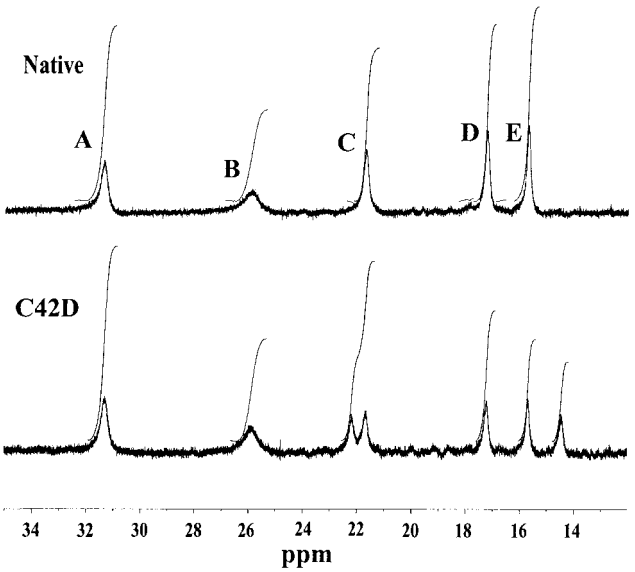

FIG. 9. **500-MHz ^{1}H NMR spectra of the oxidized native and C42D FdI.** The spectra were obtained at the room temperature using 90° pulse of 8 μs with 0.5-s delay times. About 6000 scans were accumulated for each spectrum over the 2.5 h. The samples were exchanged into a 50 mM Tris-buffered D_2O solution, pH 7.8, by passage through a Sephadex G-25 column (1.5 × 15 cm) and then concentrated to ~0.6–1.0 mM

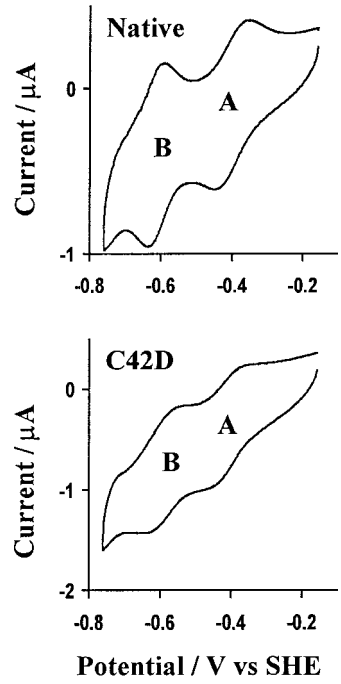

FIG. 10. **Bulk solution voltammetry of native and C42D *Av*FdI.** Protein samples were suspended in 60 mM mixed buffer, 0.1 M NaCl, and 4 mM neomycin at 0 °C, pH 7.0, scan rate 5 mV s^{-1}. Voltammograms measured on the third cycle. The concentration of C42D was lower than that of native FdI; hence, the currents are smaller.

tons of $[4Fe\text{-}4S]^{2+}$ cluster ligands. Cheng *et al.* (67) have shown that for native FdI, resonances A–C are pH-dependent, with essentially identical p*K* values of ~5.4. This pH dependence has been assigned to a non-liganded Asp^{15} near the $[3Fe\text{-}4S]^{+}$ cluster (67). A sequence-specific assignment of resonances D and E has not clearly been made for *A. vinelandii* FdI; however, by analogy to a homologous ferredoxin from *Bacillus schlegelii* (68, 69), it is probable that resonance D arises from β-CH_2 protons from Cys^{42}, the residue of interest in this study, and that resonance E arises from β-CH_2 protons from Cys^{45}. This assignment is supported by the observation of weak dipole contacts between the β-CH_2 protons of Cys^{16} in the $[3Fe\text{-}4S]^{+}$ cluster and the β-CH_2 protons of Cys^{45} that ligates $[4Fe\text{-}4S]^{2+}$, together with the observation in the ^{1}H NMR structure of a nuclear Overhauser effect between signals C and E (66, 67). As shown in Fig. 9, the spectrum of C42D indicates that replacement of ligand Cys^{42} by Asp perturbs the structures of both the Cys^{42} site and the Cys^{45} site, which results in one new signal appearing at 14.4 ppm. This perturbation at Cys^{45} is observed in the x-ray structure described above (Fig. 8, *A* and *B*). This perturbation also gives rise to a splitting of the Cys^{16} signal into two equal components with half-intensities. The substitution, however, does not change the other β-CH_2 ligand resonances for the $[3Fe\text{-}4S]^{+}$ cluster, as seen in the same chemical shifts for signals A and B.

Reduction of the $[4Fe\text{-}4S]^{2+}$ Cluster of C42D Versus Native FdI—The $[4Fe\text{-}4S]^{2+/+}$ cluster of native FdI has an unusually low reduction potential and cannot be reduced by dithionite at neutral pH. Previous studies have established, however, that it can be reduced using direct electrochemical methods (47). Fig. 10 shows bulk solution voltammetry of C42D *Av*FdI at pH 7.0. Couple A arises from $[3Fe\text{-}4S]^{+/0}$, whereas couple B arises from $[4Fe\text{-}4S]^{2+/+}$, confirming again that the cluster composition of native and C42D FdI are the same. Examination of the data in Fig. 10 shows a shift of +30 mV in the reduction potential of the $[4Fe\text{-}4S]^{2+/+}$ couple; from −0.620 V (for native FdI) to −0.590 V (for C42D FdI) *versus* standard hydrogen electrode. As expected, there was no change in the reduction potential of the $[3Fe\text{-}4S]^{+/0}$ cluster, which is remote from the site of the mutation (60). The observation that the reduction potential of the $[4Fe\text{-}4S]^{2+/+}$ cluster of C42D FdI is similar to that in native FdI is not unexpected. Thus, as shown in Table II, mutagenesis of other ferredoxins where a naturally occurring Cys-*X*-*X*-Asp-*X*-*X*-Cys motif is changed to Cys-*X*-*X*-Cys-*X*-*X*-Cys also resulted in only minor changes in reduction potential (36, 71).

In most cases, reduced $[4Fe\text{-}4S]^{+}$ clusters that have four cysteine ligands exhibit g_{av} ~1.94 signals that arise from an S = 1/2 ground state. This is true not only for naturally occurring ferredoxins but also for variants that have been constructed by mutagenesis where naturally occurring Cys-*X*-*X*-Asp-*X*-*X*-Cys motifs have been converted to Cys-*X*-*X*-Cys-*X*-*X*-Cys motifs (36, 71). In contrast, where information is available, naturally occurring reduced ferredoxins that contain $[4Fe\text{-}4S]^{+}$ cluster ligated by three cysteine and one aspartate ligands exhibit a $g \sim 5.3$ signal that arises from the ground state $m_s = \pm 3/2$. In some cases, these clusters exhibit only the S = 3/2 spin state (for example, *Da*FdIII (Refs. 25, 72, and 73) and an A33Y mutant of *Pf*Fd (Ref. 74)), whereas, in others, they exhibit a mixture of S = 1/2 and S = 3/2 states (23, 71). In order to compare the spectra of the reduced $[4Fe\text{-}4S]^{+}$ clusters in C42D and native FdI, a low reduction potential system was employed, utilizing the photoreduction of 5′-deazariboflavin with EDTA as sacrificial electron donor. As shown in Fig. 11*A*, the reduced $[4Fe\text{-}4S]^{+}$ cluster of C42D FdI exhibits an S = 1/2 EPR signal with resonances, g = 2.14, 1.86, and 1.79. The signal is much broader than that observed for the native protein. The same extent of signal broadness has been reported previously for other oxygen-liganded proteins, substrate-complexed aconitase[2] (75), aspartate-liganded *Pf*Fd (76), and probably OH^--

[2] In substrate-bound aconitase, both H_2O and the carboxylate group of substrate are also bound to one iron of [4Fe-4S] cluster. Unlike C42D FdI, the fourth iron is easily lost upon exposure to air. In addition to signal broadening, there is a distinct shift in g-values when substrate binds to reduced aconitase with bound g-values of 2.04, 1.85, and 1.78, which compares with reduced C42D FdI with 2.14, 1.86, and 1.79. Aconitase without substrate-bound is 2.06, 1.93, and 1.86.

TABLE II
The comparison of reduction potentials for Cys-X-X-Cys-X-X-Cys versus Cys-X-X-Asp-X-X-Cys in the same protein

Both *Da*FdIII and *Pf*Fd mutants have Cys instead of Asp in the Cys-*X*-X-Asp-*X*-X-Cys motif, whereas C42D FdI has Asp instead of Cys in the Cys-*X*-X-Cys-*X*-X-Cys motif.

	$E^{0\prime}$ (mV *vs.* SHE)		$\Delta E^{0\prime}$ ($E^{0\prime}_{Cys} - E^{0\prime}_{Asp}$)	Reference
	Cys	Asp		
			mV	
*Da*FdIII	−425	−400	−25	36
*Pf*Fd	−422	−375	−47	71
*Av*FdI	−620	−590	−30	This work

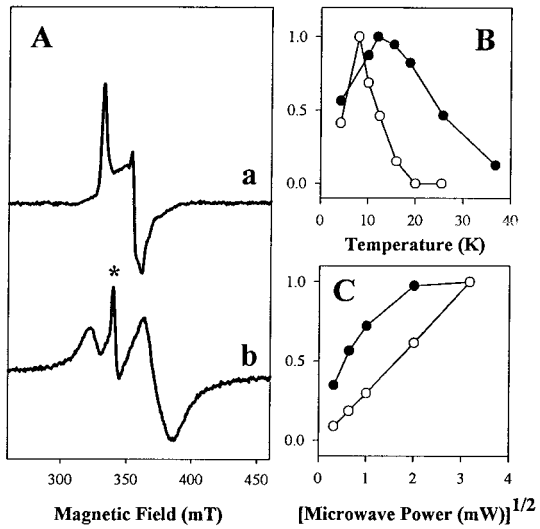

FIG. 11. **EPR spectra (*A*), temperature dependence at 1 mW microwave power (*B*), and power dependence at 10 K (*C*) for reduced [4Fe-4S]$^+$ cluster of native and C42D *Av*FdI.** The reduction of FdI was carried out by mixing degassed FdI, 5′-deazariboflavin, and EDTA (final concentration, 0.2, 0.15, and 10 mM, respectively) in 0.05 M Tris-HCl, pH 8.0, and then illuminating for 1 min using white light from fiber optics illuminator model 20. *A*, *a*, native FdI; *b*, C42D FdI. *B* and *C*, *closed circle*, native FdI; *open circle*, C42D FdI. Conditions of measurements: microwave frequency, 9.59 GHz; modulation amplitude, 0.64 mT; microwave power, 1 mW; temperature, 10 K; receiver gain, 2×10^4. This reduction system is light-dependent and difficult to control. For the experiment shown, 50% of the native [4Fe-4S]$^{2+/+}$ and 34% of the C42D [4Fe-4S]$^{2+/+}$ cluster were reduced. Note that for C42D, some oxidized [3Fe-4S] cluster is still present, as indicated by the *asterisk* (*).

liganded dihydroxy-acid dehydratase (77). As shown in Fig. 11 (*B* and *C*), the C42D non-cysteine-liganded S = 1/2 [4Fe-4S]$^+$ resonance undergoes more rapid relaxation than the cysteine-only native [4Fe-4S]$^+$ resonance since it is not observable at temperatures above 18 K and it is not easily saturated. One striking aspect is that no S = 3/2 or other high spin signals were detected for 200 μM C42D FdI under the conditions that were adjusted in temperature from 4.2 K to 30 K and/or in microwave power from 0.1 mW to 100 mW.

The [4Fe-4S]$^{2+/+}$ cluster of C42D FdI is the only known example of an O_2-stable 4Fe cluster with one aspartate and three cysteine ligands. The above data show that it is also the only example so far established of a cluster of that type that is exclusively S = 1/2 in the reduced state. This result suggests that the prior observation of S = 3/2 EPR for aspartate-liganded [4Fe-4S]$^+$ clusters is not due to the aspartate ligand *per se* but rather to some other property of the cluster. One property that may unite the easily convertible, O_2-sensitive, and S = 3/2 clusters is their accessibility to solvent. In this regard, we note that the [4Fe-4S]$^+$ cluster of the Fe protein of nitrogenase is solvent-exposed, extremely oxygen-sensitive, and exhibits a mixed S = 1/2 and S = 3/2 spin state despite the fact that it has four cysteine ligands rather than three cysteine and one aspartate (78). There are several reports in the literature showing that spin crossover is solvent-induced (23, 79–85). For the nitrogenase Fe protein, the addition of a denaturing agent such as 0.4 M urea stabilizes the S = 3/2 state, whereas both 50% (v/v) ethylene glycol and glycerol favor the S = 1/2 spin state (79). In *Pf*Fd, 50% (v/v) glycerol, but not 0.4 M urea affects the relative populations of the S = 1/2 and S = 3/2 states and results in a shift in favor of the S = 1/2 species (23). Solvents such as acetonitrile or dimethyl sulfoxide also induce spin mixtures in the synthetic analog $[Fe_4S_4(SR)_4]^{3-}$ (R = alkyl or aryl) (80). Finally, the 2[4Fe-4S]$^{2+/+}$ PsaC protein mutants, C14D and C51D, are also known to be easily converted from S = 3/2 to S = 1/2 at the modified cluster upon binding to the photosystem I core complex, a situation that is likely to affect solvent accessibility (81–85).

Interestingly, there are several examples of other proteins showing S > 1/2 spin states with cysteine-only ligated [4Fe-4S]$^{2+/+}$ clusters. For example, the *Bacillus subtilis* glutamine phosphoribosylpyrophosphate aminotransferase has the S = 3/2 [4Fe-4S]$^+$ as the dominant species and S = 1/2 and 5/2 as minor components (86). In *Thauera aromatica* ferredoxin, which contains cysteine only-ligated 2[4Fe-4S]$^{2+/+}$ clusters, a spin mixture of S = 3/2 and 5/2 is observed for one cluster in the reduced state (87). Structures are not yet available for these clusters, and their solvent accessibility has not been reported.

The [4Fe-4S]$^{2+/+}$ Cluster of C42D FdI Is Extremely Stable and Is Not Converted to a [3Fe-4S]$^{+/0}$ Cluster by Conventional Methods—As shown above, like native FdI, C42D FdI is a completely air-stable protein that contains one [3Fe-4S]$^{+/0}$ cluster and one [4Fe-4S]$^{2+/+}$ cluster. This is the only known example of a [4Fe-4S]$^{2+/+}$ cluster with three cysteines and one water or aspartate ligand that is not converted to a [3Fe-4S]$^{+/0}$ cluster upon exposure to oxygen. We therefore attempted to do the conversion using alternative methods that had been successful with other proteins. One of these methods involves addition of potassium ferricyanide (10, 88–91). However, in the case of C42D FdI, addition of $Fe(CN)_6^{3-}$ did not result in cluster conversion, as monitored by quantitative examination of the g = 2.01 signal that arises from the [3Fe-4S]$^+$ clusters. A successful conversion should have doubled the size of that signal, but, as shown in Fig. 7, the [3Fe-4S]$^+$ signal exhibited by C42D FdI was both qualitatively and quantitatively unchanged following the addition of ferricyanide.

In studies of *Da*FdIII, it was demonstrated that externally added thiolates could compete with the easily displaced aspartate ligand to form [4Fe-4S]$^{2+/+}$ clusters with three endogenous cysteine ligands and one exogenous thiolate ligand (92). The products could be easily identified using direct electrochemical methods because their reduction potentials were significantly different from that of the original cluster. For example, the transformed (O_2-sensitive) [4Fe-4S]$^{2+/+}$ cluster in *Da*FdIII coordinates exogenous 2-mercaptoethanol as a ligand, whereupon its reduction potential becomes approximately 190 mV more negative. By contrast, no such shift in reduction potential was observed for C42D FdI when an electrode coated with a protein film was placed in a buffered solution of 715 mM 2-mercaptoethanol at pH 8.0. Thus, all of our attempts to use conventional methods to displace the aspartate ligand of C42D FdI were unsuccessful, thus demonstrating the extreme stability of this cluster.

Conversion of the C42D FdI [4Fe-4S] Cluster to a [3Fe-4S] Cluster Was Ultimately Accomplished Using a New Electrochemical Method—The mechanism of the 4Fe to 3Fe cluster conversion reaction in any protein has yet to be established but,

as shown in Reaction I, it has been suggested to involve transient oxidation of the $[4Fe\text{-}4S]^{2+}$ cluster to the superoxidized HiPIP $[4Fe\text{-}4S]^{3+}$ state prior to removal of iron (75, 93–95).

$$[4Fe\text{-}4S]^{2+} \rightarrow \{[4Fe\text{-}4S]^{3+}\} \rightarrow [3Fe\text{-}4S]^{+}$$

REACTION I

This possibility has recently been studied using direct electrochemical methods with *Clostridium pasteurianum* Fd, which contains two $[4Fe\text{-}4S]^{2+/+}$ clusters with complete cysteine ligation. The experiment, which is discussed in detail elsewhere (96), involves subjecting a protein film at an electrode surface to short pulses (*e.g.* 0.1 to 4 s) at various high potentials to create the superoxidized $[4Fe\text{-}4S]^{3+}$ state. This species is usually unstable and breaks up, but it is possible to optimize conditions (pulse potential and duration) to control this oxidative fragmentation, so that just one iron atom is ejected, thus forming a [3Fe-4S] cluster. The success of the experiment is easily monitored by immediate cyclic voltammetry of the same film because the new [3Fe-4S] cluster exhibits two signals. One, designated A′, arises from the $[3Fe\text{-}4S]^{+/0}$ transition; the other, designated C′, which is more prominent, arises from a further two-electron $[3Fe\text{-}4S]^{0/2-}$ transition.

The above method was successful in converting both of the two $[4Fe\text{-}4S]^{2+/+}$ clusters of *C. pasteurianum* Fd to a [3Fe-4S] cluster, even though the original clusters each have four cysteine ligands. This method, however, has not so far been successful in converting the $[4Fe\text{-}4S]^{2+/+}$ cluster of native FdI. Although the $[4Fe\text{-}4S]^{2+/+}$ cluster of C42D FdI is extremely stable when compared with aspartate-ligated clusters in other proteins, we thought that it might be less stable than the cluster in native FdI. To test this, a variety of pulse times, pulse potentials, and other conditions were used. Optimum formation of new signals attributable to a second [3Fe-4S] cluster was observed when a film of C42D FdI was poised, at pH 8.0, at a potential of +0.643 V for 4 s, 3 s, and finally 2 s with voltammograms recorded between each poise. The result is shown in Fig. 12. The 7Fe protein that is present at the start of the experiment (Fig. 12*A*, *top panel*) clearly shows three signals, A′, B′, and C′, corresponding to the $[3Fe\text{-}4S]^{+/0}$, $[4Fe\text{-}4S]^{2+/+}$, and $[3Fe\text{-}4S]^{0/-2}$ redox couples, respectively (97). As is commonly found in the film voltammetry of [3Fe-4S]-cluster-containing proteins, the C′ signal is kinetically complex and displays a large peak separation; thus, even at a relatively slow scan rate of 50 mV s^{-1}, the C′ peak overlaps the B′ peak in the oxidative scan whereas they are clearly separated in the reducing direction. Fig. 12*A* (*bottom panel*) shows the voltammetry of the product; the B′ couple that arises from the indigenous $[4Fe\text{-}4S]^{2+/+}$ cluster has disappeared and has been replaced by two new signals labeled A*′ and C*′. Their appearance is fully consistent with the formation of a second [3Fe-4S] cluster.

The change in ratios A′/C′ after the pulse probably arises because application of high potentials also causes extensive desorption of the protein from the electrode surface (96). The desorbed ferredoxin molecules, many of which will escape without undergoing the cluster transformation, are initially still able to diffuse back to the electrode and undergo electron transfer, but without becoming adsorbed. The A′ and C′ signals in a diffusional voltammogram do not reflect the expected 1-to-2 stoichiometry, *i.e.* the C′ signal is rarely observed unless the protein is tightly bound to the electrode. (This is most likely due to the complexity of the cooperative two-electron redox reaction, which involves sequential electron-proton transfers that require a sufficiently long residence time at the electrode (Ref. 97).)

Fig. 12*B* compares the pH dependence of the reduction potentials of the new and indigenous [3Fe-4S] cluster signals for

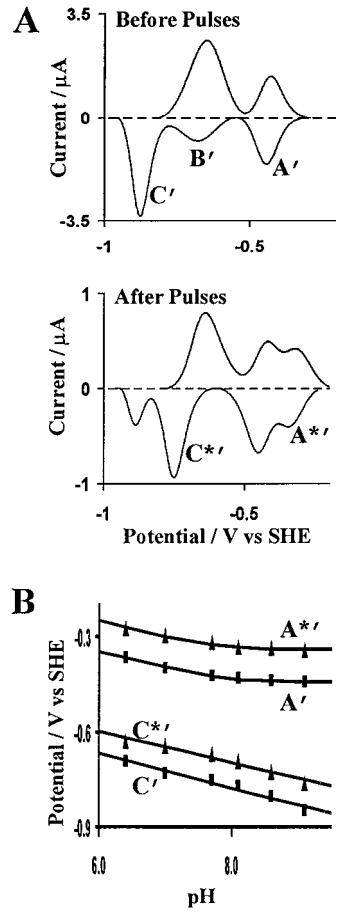

FIG. 12. *A*, base-line subtracted film voltammograms of C42D *Av*FdI measured before (*top panel*) and after (*bottom panel*) poising at a potential of +0.643 V for 4, 3 and then 2 s, at pH 8.0, 0 °C. *B*, plots of $E^{0'}$ *versus* pH for the new (▲) and indigenous (■) [3Fe-4S] cluster A′ and C′ couples. Film solution contains approximately 100 μM protein in 60 mM mixed buffer, 0.1 M NaCl, and 200 μg/ml polymyxin at pH 7.0. Cell solutions were similar to the film solution, but contained no protein and was at the required pH.

C42D FdI. The slopes for both redox couples and their pK_a values are similar for both clusters, with the new A′ couple having pK_a = 7.7 and E_{alk} = −0.341V. The pK_a arises from coupled proton-electron transfer reactions that are well characterized for the native protein (97). The reduction potential of the new $[3Fe\text{-}4S]^{+/0}$ cluster is about 100 mV more positive than that of the indigenous cluster. This is not surprising since $[3Fe\text{-}4S]^{+/0}$ clusters in different proteins vary greatly in their reduction potentials.

Even though we were successful in converting the 4Fe cluster of C42D FdI to a 3Fe cluster by electrochemical pulsing, the product could not be readily converted back to a 4Fe cluster. Thus, unlike the situation with easily converted clusters (70, 98), when films of the 6Fe form of C42D FdI were placed in 5 mM solutions of Fe^{2+}, Zn^{2+}, and Tl^{+}, no signs of metal uptake were observed.

Why Can't the C42D FdI $[4Fe\text{-}4S]^{2+/+}$ Cluster Be Easily Converted to a $[3Fe\text{-}4S]^{+/0}$ Cluster?—Taken together, the above data demonstrate that it is not the presence of an aspartate ligand in the central position *per se* that allows the facile conversion of a $[4Fe\text{-}4S]^{2+/+}$ cluster to a $[3Fe\text{-}4S]^{+/0}$ cluster upon oxygen and ferricyanide addition. Fig. 8 (*A* and *B*) shows the structure for the $[4Fe\text{-}4S]^{2+/+}$ cluster region of C42D FdI. The aspartate fits tightly and is held in place and restrained by van der Waals contacts with the three hydrophobic residues Ile^{40}, Leu^{44}, and Pro^{21}. These interactions would be expected to

limit access of solvent to the [4Fe-4S]$^{2+/+}$ cluster at the site of Asp^{42} ligation, and at the same time prevent dissociation of the aspartate from the cluster. Although the carboxylate carries the same negative charge as a cysteine ligand, its oxygen atoms are less polarizable than sulfur. The negative charge, within the hydrophobic cavity formed by Pro^{21}, Ile^{40}, and Leu^{44}, is compensated not only by the [4Fe-4S]$^{2+}$ cluster, but also by two electrostatic interactions, one involving Oδ2 with the amide of Leu^{44}, and the other Oδ1 with Pro^{21} (Fig. 8*A*). The former interaction has good geometry for a hydrogen bond, and the latter, justified by the positions of the residues in the electron density, may represent a CH . . . O hydrogen bond. Alternatively, Oδ1 of Asp^{42} may be protonated. Together, these hydrophobic contacts and electrostatic interactions help account for the stability of Asp^{42} as a ligand.

Examination of the sequences of the easily convertible proteins (Fig. 2) with a central aspartate shows that in most cases the residue at position 44 is much smaller and/or not hydrophobic, which may facilitate the movement of the aspartate. An exception is *Pf*Fd, which does easily convert, albeit at a slower rate than for *Da*FdIII (70), and has a hydrophobic Ile at the position homologous to the FdI residue number 44. Thus, although the residue 44 may be important in facilitating the cluster conversion, it cannot be the controlling factor. In order for the cluster conversion to occur, the backbone must be able to move to allow the aspartate to move away from the cluster. Examination of the sequences of the easily convertible proteins (Fig. 2) shows that, without exception, those proteins that have a central aspartate have a glycine on one or both sides of the aspartate to facilitate this backbone movement. In contrast, the Asp^{42} residue of C42D FdI is flanked by aspartate and alanine, which restrict the corresponding backbone movement. Future experiments could therefore test the hypothesis that construction of a D41G/C42D double mutant in FdI ought therefore to lead to an easily convertible cluster or that conversion of the homologous Gly^{41} position in *Pf*Fd to an aspartate would lead to a [4Fe-4S]$^{2+/+}$ cluster that could no longer be converted to [3Fe-4S]$^{+/0}$.

Acknowledgements—We thank Professor Gordon Tollin (Department of Chemistry, University of Arizona, Tucson, AZ) for generously providing 5′-deazariboflavin, and Raul Camba for advice on carrying out the protein film pulse experiments. We also thank Professor Thomas L. Poulos and Dr. Huiying Li for support in carrying out x-ray crystallography.

REFERENCES

1. Beinert, H., Holm, R. H., and Münck, E. (1997) *Science* **277,** 653–659
2. Beinert, H. (2000) *J. Biol. Inorg. Chem.* **5,** 2–15
3. Holm, R. H., Kennepohl, P., and Solomon, E. I. (1996) *Chem. Rev.* **96,** 2239–2314
4. Johnson, M. K. (1994) in *Encyclopedia of Inorganic Chemistry* (King, R. B., ed.) Vol. 4, pp. 1896–1915, Wiley Interscience, New York
5. Cammack, R. (1992) *Adv. Inorg. Chem.* **38,** 281–322
6. Howard, J. B., and Rees, D. C. (1991) *Adv. Protein Chem.* **42,** 199–280
7. Beinert, H. (1990) *FASEB J.* **4,** 2483–2491
8. Lindahl, P. A., and Kovacs, J. A. (1990) *J. Cluster Sci.* **1,** 29–73
9. Kent, T. A., Emptage, M. H., Merkle, H., Kennedy, M. C., Beinert, H., and Münck, E. (1985) *J. Biol. Chem.* **260,** 6871–6881
10. Moura, J. J. G., Moura, I., Kent, T. A., Lipscomb, J. D., Huyng, B. H., LeGall, J., Xavier, A. V., and Münck, E. (1982) *J. Biol. Chem.* **257,** 6259–6267
11. Moura, J. J. G., LeGall, J., and Xavier, A. V. (1984) *Eur. J. Biochem.* **141,** 319–322
12. Khoroshilova, N., Popescu, C., Münck, E., Beinerts, H., and Kiley, P. J. (1997) *Proc. Natl. Acad. Sci. U. S. A.* **94,** 6087–6092
13. Jordan, P. A., Thomson, A. J., Ralph, E. T., Guest, J. R., and Green, J. (1997) *FEBS Lett.* **416,** 349–352
14. Coldren, C. D., Hellinga, H. W., and Caradonna, J. P. (1997) *Proc. Natl. Acad. Sci. U. S. A.* **94,** 6635–6640
15. Gibney, B. R., Mulholland, S. E., Rabanal, F., and Dutton, P. L. (1996) *Proc. Natl. Acad. Sci. U. S. A.* **93,** 1541–1546
16. Bian, S., and Cowan, J. B. (1998) *J. Am. Chem. Soc.* **120,** 3532–3533
17. Graves, M. C., Mullenbach, G. T., and Rabinowitz, J. C. (1985) *Proc. Natl. Acad. Sci. U. S. A.* **82,** 1653–1657
18. Morgan, T. V., Lundell, D. J., and Burgess, B. K. (1988) *J. Biol. Chem.* **263,** 1370–1375
19. Okawanara, N., Ogata, M., Yagi, T., Wakabayashi, S., and Matsubara, H. (1988) *J. Biochem.* (*Tokyo*) **104,** 196–199
20. Bovier-Lapierre, G., Bruschi, M., Bonicel, J., and Hatchikian, E. C. (1987) *Biochim. Biophys. Acta* **913,** 20–26
21. Minami, Y., Wakabayashi, S., Wada, K., Matsubara, H., Kerscher, L., and Oesterhelt, D. (1985) *J. Biochem.* (*Tokyo*) **97,** 745–753
22. Wakabayashi, S., Fujimoto, N., Wada, K., Matsubara, H., Kerscher, L., and Oesterhelt, D. (1983) *FEBS Lett.* **162,** 21–24
23. Conover, R. C., Kowal, A. T., Fu, W., Park, J.-B., Aono, S., Adams, M. W. W., and Johnson, M. K. (1990) *J. Biol. Chem.* **265,** 8533–8541
24. Wakagi, T., Fujii, T., and Oshima, T. (1996) *Biochem. Biophys. Res. Commun.* **225,** 489–493
25. George, S. J., Armstrong, F. A., Hatchikian, E. C., and Thomson, A. J. (1989) *Biochem. J.* **264,** 275–284
26. Thomson, A. J., Breton, J., Butt, J. N., Hatchikian, E. C., and Armstrong, F. A. (1992) *J. Inorg. Biochem.* **47,** 197–207
27. Gorst, C. M., Yeh, Y. H., Teng, Q., Calzolai, L., Zhou, Z. H., Adams, M. W. W., and La Mar, G. N. (1995) *Biochemistry* **34,** 600–610
28. Calzolai, L., Gorst, C. M., Zhou, Z. H., Teng, Q., Adams, M. W. W., and La Mar, G. N. (1995) *Biochemistry* **34,** 11373–11384
29. Calzolai, L., Zhou, Z. H., Adams, M. W. W., and La Mar, G. N. (1996) *J. Am. Chem. Soc.* **118,** 2513–2514
30. Kissinger, C. R., Sieker, L. C., Adman, E. T., and Jensen, L. H. (1991) *J. Mol. Biol.* **219,** 693–715
31. Robbins, A. H., and Stout, C. D. (1989) *Proc. Natl. Acad. Sci. U. S. A.* **86,** 3639–3643
32. Robbins, A. H., and Stout, C. D. (1989) *Proteins* **5,** 289–312
33. Reyntjens, B., Jollie, D. R., Stephens, P. J., Gao-Sheridan, H. S., and Burgess, B. K. (1997) *J. Biol. Inorg. Chem.* **2,** 595–602
34. Gao-Sheridan, H. S., Pershad, H. R., Armstrong, F. A., and Burgess, B. K. (1998) *J. Biol. Chem.* **273,** 5514–5519
35. Mandori, A., Cecchini, G., Schröder, I., Gunsalus, R. P., Werth, M. T., and Johnson, M. K. (1992) *Biochemistry* **31,** 2703–2712
36. Busch, J. L., Breton, J. L., Bartlett, B. M., Armstrong, F. A., James, R., and Thomson, A. J. (1997) *Biochem. J.* **323,** 95–102
37. Thomson, A. J., Robinson, A. E., Johnson, M. K., Cammack, R., Rao, K. K., and Hall, D. O. (1981) *Biochim. Biophys. Acta* **637,** 423–432
38. Sridhar, V., Prasad, G. S., Burgess, B. K., and Stout, C. D. (1998) *J. Biol. Inorg. Chem.* **3,** 140–149
39. Morgan, T. V., Stephens, P. J., Devlin, F., Stout, C. D., Melis, K. A., and Burgess, B. K. (1984) *Proc. Natl. Acad. Sci. U. S. A.* **81,** 1931–1935
40. Morgan, T. V., Stephens, P. J., Devlin, F., Burgess, B. K., and Stout, C. D. (1985) *FEBS Lett.* **183,** 206–210
41. Gao-Sheridan, H. S. (1998) Engineering [Fe-S] Cluster Composition and Ligand Coordination in *Azotobacter vinelandii* Ferredoxin I. Ph.D. thesis, University of California, Irvine, CA
42. Shen, B., Martin, L. L., Butt, J. N., Armstrong, F. A., Stout, C. D., Jensen, G. M., Stephens, P. J., La Mar, G. N., Gorst, C. M., and Burgess, B. K. (1993) *J. Biol. Chem.* **268,** 25928–25939
43. Vázquez, A., Shen, B., Negaard, K., Iismaa, S., and Burgess B. (1994) *Protein Exp. Purif.* **5,** 96–102
44. Jung, Y.-S., Gao-Sheridan, H. S., Christiansen, J., Dean, D. R., and Burgess, B. K. (1999) *J. Biol. Chem.* **274,** 32402–32410
45. Burgess, B. K., Jacobs, D. B., and Stiefel, E. I. (1980) *Biochim. Biophys. Acta* **614,** 196–209
46. Aasa, R., and Vänngård, T. (1975) *J. Magn. Reson.* **19,** 308–315
47. Armstrong, F. A., Butt, J. N., and Sucheta, A. (1993) *Methods Enzymol.* **227,** 479–500
48. Heering, H. A., Weiner, J. H., and Armstrong, F. A. (1998) *J. Am. Chem. Soc.* **120,** 11628–11636
49. Stout, C. D. (1989) *J. Mol. Biol.* **205,** 545–555
50. Shen, B., Jollie, D. R., Diller, T. C., Stout, C. D., Stephens, P. J., and Burgess, B. K. (1995) *Proc. Natl. Acad. Sci. U. S. A.* **92,** 10064–10068
51. Brünger, A. T., Karplus, M., and Petsko, G. A. (1989) *Acta Crystallogr. A* **45,** 50–61
52. McRee, D. E. (1999) *J. Struct. Biol.* **125,** 156–165
53. Isas, J. M., and Burgess, B. K. (1994) *J. Biol. Chem.* **269,** 19404–19409
54. Isas, J. M., Yannone, S. M., and Burgess, B. K. (1995) *J. Biol. Chem.* **270,** 21258–21263
55. Yannone, S. M., and Burgess, B. K. (1997) *J. Biol. Chem.* **272,** 14454–14458
56. Yannone, S. M., and Burgess, B. K. (1998) *J. Biol. Inorg. Chem.* **3,** 253–258
57. Jung, Y.-S., Roberts, V. A., Stout, C. D., and Burgess, B. K. (1999) *J. Biol. Chem.* **274,** 2978–2987
58. Regström, K., Sauge-Merle, S., Chen, K., and Burgess, B. K. (1999) *Proc. Natl. Acad. Sci. U. S. A.* **96,** 12389–12393
59. Martin, A. E., Burgess, B. K., Iismaa, S. E., Smart, M. R., Jacobson, M. R., and Dean, D. R. (1989) *J. Bacteriol.* **171,** 3162–3167
60. Shen, B., Jollie, D. R., Stout, C. D., Diller, T. C., Armstrong, F. A., Gorst, C. M., La Mar, G. N., Stephens, P. J., and Burgess, B. K. (1994) *J. Biol. Chem.* **269,** 8564–8575
61. Iismaa, S. E., Vázquez, A. E., Jensen, G. M., Stephens, P. J., Butt, J. N., Armstrong, F. A., and Burgess, B. K. (1991) *J. Biol. Chem.* **266,** 21563–21571
62. Stout, G. H., Turley, S., Sieker, L. C., and Jensen, L. H. (1988) *Proc. Natl. Acad. Sci. U. S. A.* **85,** 1020–1022
63. Stout, C. D. (1988) *J. Biol. Chem.* **263,** 9256–9260
64. Martin, A. E., Burgess, B. K., Stout, C. D., Cash, V. L., Dean, D. R., Jensen, G. M., and Stephens, P. J. (1990) *Proc. Natl. Acad. Sci. U. S. A.* **87,** 598–602
65. Weigel, J. A., and Holm, R. H. (1991) *J. Am. Chem. Soc.* **113,** 4184–4191
66. Cheng, H., Grohmann, K., and Sweeney, W. (1990) *J. Biol. Chem.* **265,** 12388–12392
67. Cheng, H., Grohmann, K., and Sweeney, W. (1992) *J. Biol. Chem.* **267,** 8073–8080
68. Aono, S., Bertini, I., Cowan, J. A., Luchinat, C., Rosato, A., and Viezzoli, M. S.

(1996) *J. Biol. Inorg. Chem.* **1,** 523–528
69. Aono, S., Bentrop, D., Bertini, I., Donaire, A., Luchinat, C., Niikura, Y., and Rosato, A. (1998) *Biochemistry* **37,** 9812–9826
70. Fawcett, S. E. J., Davis, D., Breton, J. L., Thomson, A. J., and Armstrong, F. A. (1998) *Biochem. J.* **335,** 357–368
71. Zhou, Z. H., and Adams, M. W. W. (1997) *Biochemistry* **36,** 10892–10900
72. Busch, J. L. H., Breton, J. L. J., Bartlett, B. M., James, R., Hatchikian, E. C., and Thomson, A. J. (1996) *Biochem. J.* **314,** 63–71
73. Busch, J. L. H., Breton, J. L., Davy S. L., James, R., Moore, G. R., Armstrong, F. A., and Thomson, A. J. (2000) *Biochem. J.* **346,** 375–384
74. Duderstadt, R. E., Brereton, P. S., Adams, M. W. W., and Johnson, M. K. (1999) *FEBS Lett.* **454,** 21–26
75. Emptage, M. H., Dreyer, J.-L., Kennedy, M. C., and Beinert, H. (1983) *J. Biol. Chem.* **258,** 11106–11111
76. Aono, S., Bryant, F. O., and Adams, M. W. W. (1989) *J. Bacteriol.* **171,** 3433–3439
77. Flint, D. H., Emptage, M. H., Finnegan, M. G., Fu, W., and Johnson, M. K. (1993) *J. Biol. Chem.* **268,** 14732–14742
78. Burgess, B. K., and Lowe, D. J. (1996) *Chem. Rev.* **96,** 2983–3011
79. Hagen, W. R., Eady, R. R., Dunham, W. R., Hakker, H. (1985) *FEBS Lett.* **189,** 250–254
80. Carney, M. J., Papaefthymiou, G. C., Spartalians, K., Frankel, R. B., and Holm, R. H. (1988) *J. Am. Chem. Soc.* **110,** 6084–6095
81. Jung, Y.-S., Vassiliev, I. R., and Golbeck, J. H. (1997) *J. Biol. Inorg. Chem.* **2,** 209–217
82. Yu, L., Bryant, D. A., and Golbeck, J. H. (1995) *Biochemistry* **34,** 7861–7868
83. Yu, L., Vassiliev, I. R., Jung, Y.-S., Bryant, D. A., and Golbeck, J. H. (1995) *J. Biol. Chem.* **270,** 28118–21125
84. Jung, Y.-S., Vassiliev, I. R., Qiao, F., Yang, F., Bryant, D. A., and Golbeck, J. H. (1996) *J. Biol. Chem.* **271,** 31135–31144
85. Jung, Y.-S., Vassiliev, I. R., Yu, J., McIntosh, L., and Golbeck, J. H. (1997) *J. Biol. Chem.* **272,** 8040–8049
86. Onate, Y. A. Vollmer, S. J. Switzer, R. L., and Johnson, M. K. (1989) *J. Biol. Chem.* **264,** 18386–18391
87. Boll, M., Fuchs, G., Tilley, G., Armstrong, F. A., and Lowe, D. J. (2000) *Biochemistry* **39,** 4929–4936
88. Kennedy, M. C., and Beinert, H (1988) *J. Biol. Chem.* **263,** 8194–8198
89. Beinert, H., and Kennedy, M. C. (1989) *Eur. J. Biochem.* **186,** 5–15
90. Bertini, I., Briganti, F., Calzolai, L., Messori, L., and Scozzafara, A. (1993) *FEBS Lett.* **332,** 268–272
91. Bell, S. H., Dickson, D. P. E., Johnson, C. E., Cammack, R., Hall, D. O., and Rao, K. K. (1982) *FEBS Lett.* **142,** 143–146
92. Butt, J. N., Sucheta, A., Armstrong, F. A., Breton, J., Thomson, A. J., and Hatchi Kian, E. C. (1993) *J. Am. Chem. Soc.* **115,** 1413–1421
93. Roth, E. K. H., and Jordanov, J. (1992) *Inorg. Chem.* **31,** 240–243
94. Tong, J., and Feinberg, B. A. (1994) *J. Biol. Chem.* **269,** 24920–24927
95. Zhou, J., Hu, Z., Munck, E., and Holm, R. H. (1996) *J. Am. Chem. Soc.* **118,** 1966–1980
96. Camba, R., and Armstrong, F. A. (2000) *Biochemistry*, **39,** 10587–10598
97. Duff, J. L. C., Breton, J. L. J., Butt, J. N., Armstrong, F. A., and Thomson, A. J. (1996) *J. Am. Chem. Soc.* **118,** 8593–8603
98. Butt, J. N., Armstrong, F. A., Breton, J., Goerge, S. J., Thomson, A. J., and Hatchikian E. C., (1991) *J. Am. Chem. Soc.* **113,** 6663–6670